JOURNAL OF GUIDANCE, CONTROL, AND DYNAMICS
Vol. 23, No. 4, July–August 2000

Design of Nonsaturating Guidance Systems

Pini Gurfil* and Mario Jodorkovsky†
RAFAEL, Ministry of Defense, 31021 Haifa, Israel
and
Moshe Guelman‡
Technion—Israel Institute of Technology, 32000 Haifa, Israel

Design of nonsaturating guidance systems is considered. Assuming linearized kinematics, a proportional navigation guidance model is introduced. The missile guidance loop discussed contains nonlinearities such as limited missile maneuverability, limited acceleration command, and constrained measured line-of-sight angular rate. A novel approach, based on input–output stability, renders design guidelines that assure operation in the nonsaturating region, given the missile–target maneuver ratio. These guidelines yield a proportional-navigation-based guidance law that assures zero miss distance for any bounded target maneuver. It is shown that if the total dynamics of the guidance loop is designed to be positive real, and the effective proportional navigation constant is chosen to be a simple function of the maneuver ratio, no saturation shall occur. The illustrative examples validate the analysis and show that the new guidance law is robust enough to guarantee a significant performance improvement even if the design guidelines are somewhat loosened.

Nomenclature

a	= lateral acceleration
L^1, L^p, L^∞	= normed space
N'	= effective proportional navigation constant
{PR}	= class of positive real (PR) functions
R	= missile–target relative range
r	= relative order of a rational function
t_f	= flight time
V	= velocity
V_C	= closing velocity
y	= missile–target relative vertical position
ζ	= damping coefficient
λ	= line-of-sight angle
μ	= bound on the required missile–target maneuver ratio
μ_r	= required missile–target maneuver ratio
μ_0	= given missile–target maneuver ratio
τ	= time to go
τ_1	= time constant
ω_n	= natural frequency
$\|\cdot\|_p$	= p norm
$\|\cdot\|_\infty$	= ∞ norm

Subscripts

C	= commanded value
f	= final value
M	= missile
T	= target
0	= initial value

Superscript

$(\dot{\cdot})$	= time differentiation

Received 22 April 1999; revision received 17 November 1999; accepted for publication 17 November 1999.

*Research Engineer, P.O. Box 2250, Department 39; pinig@rafael.co.il. Member AIAA.
†Senior Research Scientist, P.O. Box 2250, Department 39; marioj@rafael.co.il.
‡Professor, Department of Aerospace Engineering; aerglmn@aerodyne.technion.ac.il.

I. Introduction

THE design of a guidance law for a given missile system is effected primarily from the a priori knowledge of the missile acceleration capability. When the missile–target maneuver ratio is known, a suitable guidance method can be synthesized. Several approaches to confront this problem have been suggested in previous studies. Based on optimal control theory, explicit formulas of optimal guidance for acceleration constrained missile were derived both for the deterministic[1] and stochastic[2] cases. The differential games approach has also been utilized.[3] In both approaches, the guidance law is sought by solving a dynamic optimization problem.

However, in many actual applications, the guidance law is chosen without performing a constrained optimization. The designer chooses the guidance law based on considerations involving the available measurements, the minimization of miss distance, and the ease of implementation. The problem of limited acceleration is then dealt with by a proper tuning of the guidance law parameters. The basic question is then whether after determining a guidance method, it can be improved such that missile acceleration (or any other state variable) saturation is avoided.

One of the most commonly used guidance laws is proportional navigation (PN). A vast amount of literature exists on the subject (e.g., see Refs. 4 and 5 and the references therein). In a conventional PN guidance (PNG) system, it is known[6–8] that an infinite missile acceleration is required near interception. This means that saturation is always reached, and miss distance will be greater than predicted by linear analysis.

Our main goal is to characterize a set of PN-based guidance systems, in which saturation is avoided. Thus, the basic guidance framework is set to be PNG, and an improvement to this guidance law is sought, such that a priori knowledge of the missile–target maneuver ratio will suffice to guarantee a nonsaturating operating region. It will be shown that this class of improved PN-based systems yields zero miss distance (ZMD) for any bounded target maneuver.

Although the general problem of PNG features nonlinear kinematics, to apply known techniques of analysis and design, the system equations are linearized, yielding an equivalent linear time-varying system. The linearization is valid when it is assumed that the missile and target approach the so-called collision course. It is known that the linearized model faithfully represents the guidance dynamics.[5,9] Based on the assumption of linearized kinematics, we introduce nonlinearities associated with acceleration saturation either in the output or the command channels. An additional nonlinearly we consider is the measured line-of-sight (LOS) angular rate saturation.

The a priori knowledge of missile–target maneuver ratio is used to characterize the PN-based guidance systems dynamics that render nonsaturating behavior. This is performed by implementing functional analysis tools, mainly the concept of bounded-input bounded-output stability in appropriate functional spaces.[10–12] Valuable design guidelines are derived that offer a simple improvement of a PNG system such that saturation is avoided. Based on previous works,[13,14] it is pointed out that when saturation is prevented, ZMD can be obtained for any bounded target maneuver. Furthermore, we show that the design guidelines could be somewhat relieved without a substantial modification of either the nonsaturating or ZMD property. The novel approach offered in this paper will be illustrated in several examples.

The paper is organized as follows. Section II presents some mathematical background in the fields of functional analysis and positive-real functions. In Sec. III, the problem of designing a nonsaturating PNG-based guidance system is introduced. Section IV gives a definition of input–output stability and discusses the appropriate theorem. In Sec. V, this theorem is applied in a PNG loop. Section VI suggests the design implications stem from the preceding discussion. Section VII expands the results to the prevention of saturation of state variables other then output maneuver acceleration. The illustrative examples of Sec. VIII are used to validate the results. In Sec. IX, some concluding remarks are outlined.

II. Mathematical Background

In the sequel, we extensively implement functional analysis. Therefore, some well-known definitions of frequently used signal and system norms are briefly presented. Let E be a linear space defined over the field of real numbers $\Re$. The following signal norms are defined[15] on appropriate subsets of E for some causal signal $x(t)$:

$$\|x\|_p \triangleq \left(\int_0^{t_f} |x(t)|^p \, \mathrm{d}t\right)^{1/p}, \qquad 1 \le p < \infty \tag{1}$$

$$\|x\|_\infty \triangleq \operatorname*{ess\,sup}_{t \in [0, t_f]} |x(t)| \tag{2}$$

where as usual, $ess \sup_{t \in [0,t_f)} |x(t)| \triangleq \inf\{k \,|\, |x(t)| \le k$ almost everywhere$\}$ (in the sequel, we use the notation sup instead of *ess* sup).

The corresponding normed spaces are denoted $L^p[0, t_f]$ and $L^\infty[0, t_f]$, respectively. Note that $x(t) \in L^p[0, t_f]$ if $x(t)$ is locally (Lebesgue) integrable, and in addition

$$\|x\|_p < \infty, \qquad p \in [1, \infty) \tag{3}$$

Accordingly, $x(t) \in L^\infty[0, t_f]$ if

$$\|x\|_\infty < \infty \tag{4}$$

We consider system norms as well. The systems are assumed linear, time invariant, causal, and finite dimensional. In the time domain, input–output models for such systems have the form of a convolution equation,

$$y = h^* u = \int_{-\infty}^{\infty} h(t-\tau) u(\tau) \, \mathrm{d}\tau \tag{5}$$

where, due to causality, $h(t) = 0$ for $t < 0$.

Let $H(s)$ denote the transfer function, the Laplace transform of $h(t)$. The following system norms are defined[16]:

$$\|h\|_1 \triangleq \int_0^\infty |h(t)| \, \mathrm{d}t \tag{6}$$

$$\|h\|_2 \triangleq \left(\int_{-\infty}^{\infty} |h(t)|^2 \, \mathrm{d}t\right)^{\frac{1}{2}} = \left(\frac{1}{2\pi}\int_{-\infty}^{\infty} |H(j\omega)|^2 \, \mathrm{d}w\right)^{\frac{1}{2}} = \|H\|_2 \tag{7}$$

$$\|H\|_\infty \triangleq \sup_{\omega \in \Re} |H(j\omega)| \tag{8}$$

The corresponding normed spaces are denoted L^1, L^2, and L^∞, respectively. The notation $h \in L^1$, $h \in L^2$, and $H \in L^\infty$ means that the system norm in the appropriate normed space is finite.

For the implementation of the stability theorem, the following definitions are required.

Definition 1: A function $h(t)\colon [0, \infty] \to \Re$ is said to satisfy $h(t) \in A_1$ if and only if

$$(1+t)h(t) \in L^1 \cap L^2 \tag{9}$$

Definition 2: A function $h(t)\colon [0, \infty] \to \Re$, with $h(t) = h_1(t) + h_2(t)$ and $H_2(s)$ the Laplace transform of $h_2(t)$, is said to satisfy $h(t) \in A_2$ if and only if

$$h_1(t) \in A_1, \; H_2(s) \tag{10}$$

is strictly proper. The analysis hereafter shall utilize the so-called positive real (PR) functions, defined as follows.

Definition 3: Some stable transfer function $H(s)$ satisfies $H(s) \in \{\mathrm{PR}\}$ if and only if

$$\mathrm{Re} H(j\omega) \ge 0, \qquad \forall \omega \in \Re \tag{11}$$

Notice that Eq. (11) is satisfied if and only if

$$-\pi/2 \le \angle H(j\omega) \le \pi/2, \qquad \forall \omega \in \Re \tag{12}$$

where $\angle H(j\omega)$ is the phase of $H(s)$.

It is known[17] that for Eq. (11) to hold it is necessary, but not sufficient, that

$$r[H(s)] = 1 \quad \text{or} \quad 0 \quad \text{or} \quad -1 \tag{13}$$

where r is the relative order of $H(s)$, that is, the degree of the denominator minus the degree of the numerator.

III. Problem Formulation

The problem of designing a nonsaturating PN-based guidance system will be addressed using a familiar formulation of a simplified PNG model. Although the three-dimensional PN interception problem is rather complicated, a considerable simplification is obtained when assuming that the lateral and longitudinal maneuver planes are decoupled by means of roll control. Thus, we shall further assume that the geometry is two dimensional.

The preceding assumption permits the formulation of a general planar intercept missile–target geometry as shown in Fig. 1. Figure 1 describes a missile employing PN to intercept a maneuvering target.

Based on Fig. 1, a linearized model of the guidance dynamics can be developed. Such a model is widely used in the analysis of PNG.[4,5,8,9] A block diagram describing it is given in Fig. 2. In this linear time-varying system, missile acceleration a_M is subtracted form target acceleration a_T to form a relative acceleration $\ddot{y}$. A double integration yields the relative vertical position y (see Fig. 1), which at the end of the engagement is the miss distance $y(t_f)$. By the assumption that the closing velocity V_C is constant, the relative range is given by

$$R = V_C \cdot \tau \tag{14}$$

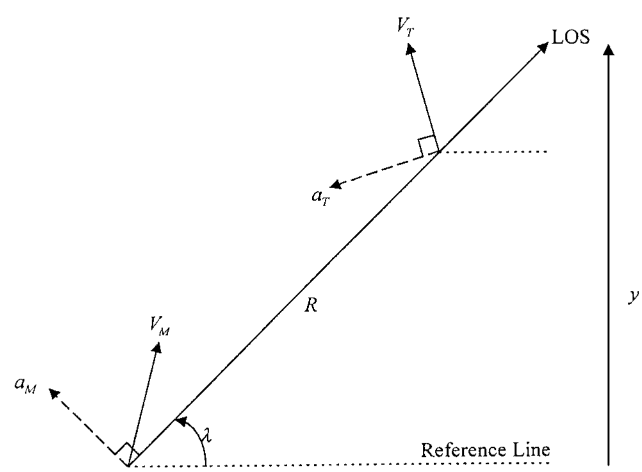

Fig. 1 Interception geometry.

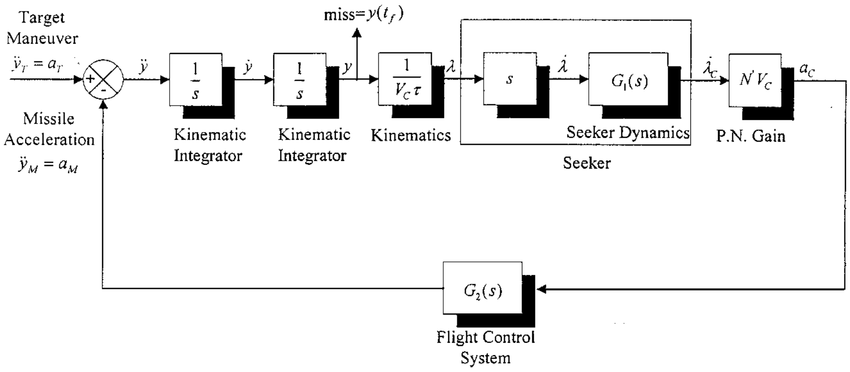

Fig. 2 Linear PNG model block diagram.

where τ is the time to go, defined as

$$\tau \triangleq t_f - t \tag{15}$$

Dividing the relative vertical position y by the range given in Eq. (14) yields the geometric LOS angle λ. It is assumed that λ is a small angle. The missile seeker is represented in Fig. 2 as an ideal differentiator with an additional transfer function $G_1(s)$, representing the LOS measurement and noise filtering dynamics. The seeker generates an LOS rate command $\dot{\lambda}_C$, which is multiplied by the PN gain $N' \cdot V_C$ to form a commanded missile maneuver acceleration a_C, with N' being the effective PN constant. The flight control system, whose dynamics are represented by the transfer function $G_2(s)$, attempts to maneuver the missile adequately to follow the desired acceleration command.

The linear model presented is based implicitly on the assumption of nonlimited missile maneuverability. Actually, every real missile system is subject to maneuverability saturation due to aerodynamic or structural constraints. To complete the guidance model description in this case, the required missile maneuver acceleration a_R is introduced. The nonlinear relationship between the actual and required missile maneuver is defined by

$$a_M = a_{M_{\max}} \operatorname{sat}\left\{a_R / a_{M_{\max}}\right\} \tag{16}$$

where

$$\operatorname{sat}(x) \triangleq \begin{cases} x & \text{if} \quad x \leq 1 \\ 1 & \text{if} \quad |x| > 1 \end{cases} \tag{17}$$

Equation (16) implicitly assumes that the limit on missile maneuverability is of the aerodynamic type due to mechanical limits of control fin deflection or to hinge moment saturation. This limit is at the output of the guidance channel, as shown in Fig. 3a. However, in many missiles the limit is imposed on the acceleration command. This limit is usually designed to be sufficiently conservative, such that an aerodynamic saturation, mentioned earlier, is not reached. In this case, the limited acceleration command is denoted a_L, where

$$a_L = a_{C_{\max}} \operatorname{sat}\left\{a_C / a_{C_{\max}}\right\} \tag{18}$$

This limit is shown in Fig. 3b.

An additional state variable of the guidance loop is usually limited: the measured LOS angular rate. This limit stems from either full-scale measurement capability of the seeker rate gyro or a maximal tracking rate. In this case (Fig. 3c), the limited LOS angular rate $\dot{\lambda}_L$ satisfies

$$\dot{\lambda}_L = \dot{\lambda}_{\max} \operatorname{sat}\{\dot{\lambda} / \dot{\lambda}_{\max}\} \tag{19}$$

In a conventional PNG system, it is known[6–8] that an infinite missile acceleration is required near to intercept ($t \to t_f$). This means that saturation is always reached, and miss distance will be greater than predicted by linear analysis. Our goal is to characterize a set of PN-based guidance systems, in which saturation is avoided. It will be shown, that this class of systems yields ZMD for any type of bounded target maneuver. The treatment hereafter will consider the case of a limited output acceleration. Nevertheless, the other types of limits mentioned will be discussed later in the study.

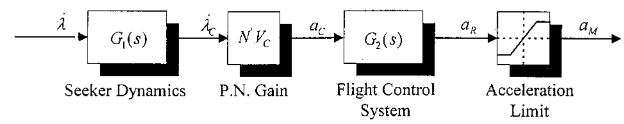

Fig. 3a Limited output acceleration.

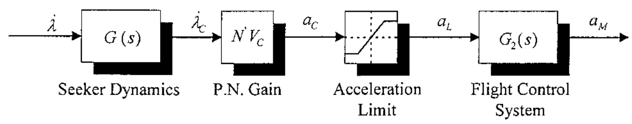

Fig. 3b Limited acceleration command.

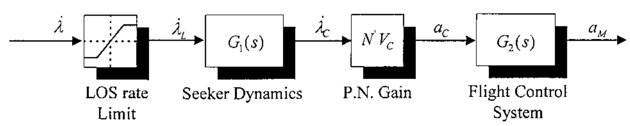

Fig. 3c Limited LOS angular rate.

Consequently, it is necessary to find some bound μ on the required missile–target maneuver ratio μ_r defined as

$$\mu_r \triangleq \frac{\sup_{t \in [0, t_f]} |a_M(t)|}{\sup_{t \in [0, t_f]} |a_T(t)|} \tag{20}$$

If μ is found to be smaller than the a priori known missile–target maneuver ratio μ_0, no saturation will occur.

In the case of PNG, due to the divergence of the state variables at the vicinity of the interception, we have $\lim_{t \to t_f} |a_M(t)| \to \infty \ \forall a_T(t) \neq 0$. We shall prove that there is a way to modify the PNG law such that $\sup_{t \in [0, t_f]} |a_M(t)| < \infty$. Moreover, we shall find a constant μ such that

$$\sup_{t \in [0, t_f]} |a_M(t)| = \|a_M(t)\|_\infty \leq \mu \|a_T(t)\|_\infty = \mu \sup_{t \in [0, t_f]} |a_T(t)| \tag{21}$$

A proper assessment of μ, together with a proper design modification of the PNG, might yield the aspired nonsaturating guidance system.

Remark 1: Clearly, μ is not uniquely defined by the preceding inequality. It is clear that we are interested in the smallest μ such that Eq. (21) still holds.

Inequality (21) describes a bounded-input bounded-output stability problem in the functional space $L^\infty[0, t_f]$. An application of this problem to a PNG loop is the main issue dealt with in the forthcoming sections.

IV. Input–Output Stability Definition and Sufficiency Theorem

Consider the nonlinear time-varying feedback system shown in Fig. 4. The input to the system is $u(t) \in \Re$ and the output is $z(t) \in \Re$. These signals are defined for $t \in [0, t_f]$. $K_1(s)$, $K_2(s)$, and $K_3(s)$ are

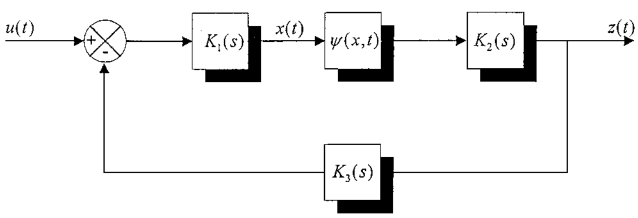

Fig. 4 Nonlinear time-varying feedback system.

linear time invariant, whereas $\psi(x, t)$ is a nonlinear time-varying operator satisfying ψ: $\Re \times \Re_{+} \rightarrow \Re$. It is assumed that $\psi(x, t)$ is a continuous sector-bounded nonlinearity, that is,

$$\alpha x(t) \leq \psi(x, t) \leq \beta x(t), \qquad \forall x(t) \in \Re, \qquad \alpha, \beta \in \Re \tag{22}$$

If $\psi(x, t) = \psi(t)x(t)$, the sector condition (22) becomes

$$\alpha \leq \psi(t) \leq \beta, \qquad \alpha, \beta \in \Re \tag{23}$$

Also, let

$$H(s) \triangleq K_1(s)K_2(s)K_3(s) \tag{24}$$

Assumption 1: $H(s)$ is stable, and its poles on the imaginary axis are distinct.

Referring to the system of Fig. 4, the following definition is used.[15]

Definition 4: The system of Fig. 4 is said to be L^∞ / L^∞ stable if and only if $u(t) \in L^\infty [0, t_f]$ implies $z(t) \in L^\infty [0, t_f]$ and, moreover,

$$\|z(t)\|_\infty \leq \mu \|u(t)\|_\infty, \qquad \forall u(t) \in L^\infty [0, t_f], \qquad \mu \neq \mu(u) \tag{25}$$

Several theorems providing sufficient conditions for L^∞ / L^∞ stability can be found in the literature.[10–12,18] The theorem we shall apply is based on the well-known small-gain theorem.[12,15] The small-gain approach states a sufficient stability condition of L^P stability of a closed-loop system, based on the L^P-induced norms of the forward and feedback paths. Thus, the nonlinearity must be confined in a sector [Eqs. (22) and (23)]. To obtain a useful result concerning the L^∞ / L^∞ stability of the PNG loop, the following formulation of the small-gain theorem is used.[12]

Theorem 1: Consider the system shown in Fig. 4. Under Assumption 1, if

$$\gamma = \frac{\beta}{2} \left\| \frac{H(j\omega)}{1 + \beta/2 \cdot H(j\omega)} \right\|_\infty \leq 1 \tag{26}$$

$$h(t) \in A_2 \tag{27}$$

then the system is L^∞ / L^∞ stable and $\|z\|_\infty \leq \mu(\gamma) \|u\|_\infty$, where the constant $\mu(\gamma)$ is, at most, a function of γ only.

Proof: See Ref. 12. □

Remark 2: A celebrated L^2 / L^2 stability theorem for the system of Fig. 4, known as the circle criterion, was obtained in Ref. 19 based on Eq. (26). It can be shown that the circle criterion is an application of the small-gain theorem.[15] However, to extend the result to L^∞ / L^∞ stability, the additional condition $e^{\varepsilon t} h(t) \in L^1 \cap L^2$, $\varepsilon > 0$, together with the shifted Nyquist plot of $H(j\omega)$ were used.[11] In a more recent work,[12] it was shown that Eq. (27) could be used as an additional condition needed for L^∞ / L^∞ stability. This condition is less conservative then previous results. Furthermore, the shifted Nyquist plot need not be used.

To clarify the relationship between Eq. (26) and the circle criterion, we consider the following lemma.

Lemma 1: Equation (26) is equivalent to the condition $\mathrm{Re}H(j\omega) \geq -(1/\beta) \forall \omega \in \Re$.

Proof: Notice that Eq. (26) can be rewritten as

$$(\beta/2)|H(j\omega)| \leq |1 + (\beta/2)H(j\omega)|, \qquad \forall \omega \in \Re \tag{28}$$

Thus,

$$\beta/2 \cdot \sqrt{\mathrm{Re}^2 H(j\omega) + \mathrm{Im}^2 H(j\omega)} \leq \sqrt{[1 + \beta/2 \cdot \mathrm{Re}H(j\omega)]^2 + [\beta/2 \cdot \mathrm{Im}H(j\omega)]^2} \qquad \forall \omega \in \Re \tag{29}$$

Simplifying both parts of the inequality yields $\mathrm{Re}H(j\omega) \geq -(1/\beta) \forall \omega \in \Re$. □

In the next section, an application of Theorem 1 and Lemma 1 in a PNG loop will be discussed.

V. Application of the Stability Theorem in a PNG Loop

One can observe that there is a complete equivalence between the problem formulated in Sec. III, especially Eq. (21), and that L^∞ / L^∞ stability definition given in regard to the system delineated in Fig. 4. Furthermore, it can be shown in a straightforward manner that a PNG loop is a particular case of the general setting.

Consider the simplified PNG loop shown in Fig. 5. The resemblance to the system of Fig. 4 is obvious:

$$u(t) = a_T(t), \qquad z(t) = a_M(t) \tag{30}$$

$$K_3(s) = 1, \qquad K_2(s) = N' \cdot s \cdot G(s), \qquad K_1(s) = 1/s^2 \tag{31}$$

$$\psi(x, t) = \psi(t) = 1/\tau = 1/(t_f - t) \in [0, \infty), \qquad \forall t \in [0, t_f) \tag{32}$$

$$H(s) = K_1(s)K_2(s)K_3(s) = N'G(s)/s \tag{33}$$

Equation (33) renders the total dynamics of the PNG loop. Restricting conditions on the transfer function $H(s)$ will be found that characterize the nonsaturating class of PN-based guidance systems.

Assumption 2: $G(0) = 1$, that is, N', is the total gain of the LTI portion of the PNG loop.

Assumption 3: $G(s)$ is asymptotically stable.

Note that the Assumption 3 does not confine the generality of the treatment. This is because $G(s)$ represents the missile closed-loop autopilot and seeker measurement dynamics, which are designed such that asymptotic stability is guaranteed.

Next, consider Eq. (26). In the case of PNG, the nonlinear time-varying element $\psi(x, t)$ reduces to a linear time-varying function (32). Note that, due to Eq. (32), this function is confined in the sector $\alpha = 0$, $\beta \rightarrow \infty$. Therefore, according to Lemma 1, Eq. (26) is satisfied if

$$\mathrm{Re}H(j\omega) = \mathrm{Re}\frac{N'G(j\omega)}{j\omega} \geq 0, \qquad \forall \omega \in \Re \tag{34}$$

or equivalently,

$$H(j\omega) \in \{\mathrm{PR}\} \tag{35}$$

Lemma 2: If Eq. (34) holds, then $\gamma = 1$.

Proof: According to Lemma 1, Eq. (34) is equivalent to Eq. (26). Thus, define

$$f(\omega) \triangleq \frac{\beta}{2} \left| \frac{H(j\omega)}{1 + \beta/2 \cdot H(j\omega)} \right| \leq 1 \tag{36}$$

Substituting $H(j\omega) = N'G(j\omega)/j\omega$ into Eq. (36) yields

$$f(\omega) = \frac{\beta}{2} \left| \frac{N'G(j\omega)}{j\omega + \beta/2 \cdot N'G(j\omega)} \right| \leq 1 \tag{37}$$

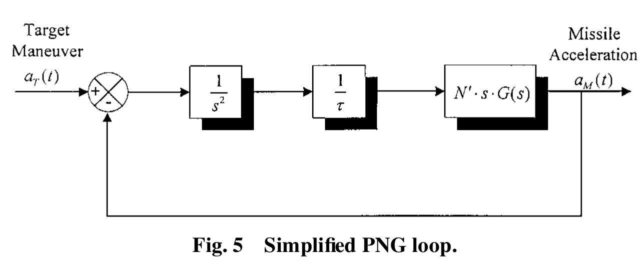

Fig. 5 Simplified PNG loop.

Recall Assumption 2. It is simple to note that assigning $\omega = 0$ into Eq. (37) yields

$$f(0) = \frac{\beta}{2}\left|\frac{N'}{\beta/2 \cdot N'}\right| = 1 \tag{38}$$

However, according to Eq. (36), $f(\omega) \leq 1$; thus, we have

$$\gamma = \frac{\beta}{2}\sup_{\omega}\left|\frac{H(j\omega)}{1 + \beta/2 \cdot H(j\omega)}\right| = f(0) = 1 \qquad \square$$

In the sequel, Lemma 2 is exploited in the derivation of the main result of the study. We proceed with the application of the additional condition of Theorem 1.

Lemma 3: Under Assumption 3 and $H(s)$ as in Eq. (33), $h(t) \in A_2$.

Proof: Assumption 3 assures that the residue of the pole $s = 0$ is 1, and so $H(s)$ can be written in the following partial fraction description:

$$H(s) = H_1(s) + N'/s \tag{39}$$

with $H_1(s)$ strictly proper. Assumption 3 also guarantees that $H_1(s)$ consists of a sum of asymptotically stable transfer functions. Therefore, $\|H_1\|_2 < \infty$ (e.g., see Ref. 16), which implies $h_1(t) \in L^2$. From the same reasons, we have $\|H_1\|_1 < \infty$ (Ref. 16). Consequently,

$$h_1(t) \in L^1 \cap L^2 \tag{40}$$

Now, it is required to show that $th_1(t) \in L^1 \cap L^2$. This will be done by applying the following characteristic of the Laplace transform:

$$\mathcal{L}[th_1(t)] = -\frac{\mathrm{d}H_1(s)}{\mathrm{d}s} \tag{41}$$

$H_1(s)$ is a rational function, that is, $H_1(s) = N(s)/D(s)$. Let $\deg[N(s)] = q$ and $\deg[D(s)] = p$. Because $H_1(s)$ is strictly proper, its relative order satisfies

$$r \triangleq p - q > 0 \tag{42}$$

Note that

$$r\left(\frac{\mathrm{d}H_1(s)}{\mathrm{d}s}\right) = r\left(\frac{\mathrm{d}N(s)/\mathrm{d}s \cdot D(s) - \mathrm{d}D(s)/\mathrm{d}s \cdot N(s)}{D^2(s)}\right)$$
$$= 2p - (q - 1 + p) = (p - q) + 1 > 0 \tag{43}$$

where the last inequality in Eq. (43) stems from Eq. (42).

Equation (43) shows that $-[\mathrm{d}H_1(s)/\mathrm{d}s]$ is strictly proper. Because $H_1(s)$ is asymptotically stable, $-[\mathrm{d}H_1(s)/\mathrm{d}s]$ is asymptotically stable as well because the differentiation does not alter the denominator polynomial. Thus, we have

$$\frac{-\mathrm{d}H_1(s)}{\mathrm{d}s} \in L^1 \cap L^2 \Rightarrow th_1(t) \in L^1 \cap L^2 \tag{44}$$

Equations (40) and (44) yield the result

$$h_1(t) \in A_1 \tag{45}$$

Now, observe Eq. (39). The term N'/s is strictly proper. Together with Eq. (45), we obtain $h(t) \in A_2$ (see Definition 2). $\square$

In the following section, the results obtained are applied to the establishment of design guidelines that prevent the guidance system saturation.

VI. Design Implications

The results obtained thus far suggested that a PNG system is L^∞/L^∞ stable provided that $H(s) \in \{\mathrm{PR}\}$. In this case, for any $a_T \in L^\infty[0, t_f]$ there exists $\mu(\gamma)$ such that $\|a_M\|_\infty \leq \mu(\gamma)\|a_T\|_\infty$. It was also proved that if $H(s) \in \{\mathrm{PR}\}$, $\gamma = 1$. To get quantitative information regarding the required missile–target maneuver ratio, $\mu(\gamma)$ should be found. Thus, the following theorem is contemplated.

Theorem 2: If $H(s) \in \{\mathrm{PR}\}$, then

$$\|a_M\|_\infty \leq \frac{N'}{N' - 2}\|a_T\|_\infty, \qquad \forall a_T \in L^\infty[0, t_f]$$

Proof: The required maneuver acceleration of a PN guided missile with ideal dynamics, that is, $G(s) = 1$ and $H(s) = 1/s$, against a constantly maneuvering target is[5]

$$\frac{a_M(t)}{a_T} = \frac{N'}{N' - 2}\left[1 - \left(1 - \frac{t}{t_f}\right)^{N'-2}\right] \tag{46}$$

Note that in this case

$$\mu(\gamma) = \frac{\sup_{t\in[0,t_f]}|a_M|}{\sup_{t\in[0,t_f]}|a_T|} = \frac{\sup_{t\in[0,t_f]}|a_M|}{a_T} = \frac{N'}{N' - 2}$$
$$\forall N' > 2, \qquad a_T = \text{const} \tag{47}$$

However, the case $H(s) = 1/s$ is a particular case of $H(s) \in \{\mathrm{PR}\}$. According to Theorem 1, $\mu(\gamma)$ is a function of γ only $\forall a_T \in L^\infty[0, t_f]$. Lemma 2 states that for any $H(s) \in \{\mathrm{PR}\}$, that is, $\mathrm{Re}H(j\omega) \geq 0\ \forall\omega \in \Re$, we have $\gamma = 1$. Thus, $\mu(\gamma)$ has the value given in Eq. (47) for any $H(s) \in \{\mathrm{PR}\}$ and $\forall a_T \in L^\infty[0, t_f]$. $\square$

The consequence of Theorem 2 should be interpreted as follows. If the PNG system is designed such that $H(s) \in \{\mathrm{PR}\}$, and $N'/(N' - 2)$ is chosen to be higher then the a priori known missile–target maneuver ratio, acceleration saturation will be avoided. This is provided that the target maneuver satisfies $a_T \in L^\infty[0, t_f]$. Nevertheless, most physical target maneuvers, such as a constant maneuver, a sinusoidal maneuver, or a bang–bang maneuver, are L^∞ bounded. Theorem 2 expands the results known in the literature because it shows that the required missile–target maneuver ratio should be $N'/(N' - 2)$ not only for an ideal missile and a constant target maneuver, but also for any missile dynamics satisfying $\mathrm{Re}H(j\omega) \geq 0\ \forall\omega \in \Re$ and any target maneuver with bounded maximal value.

It is desirable to formulate the condition $H(s) \in \{\mathrm{PR}\}$ in terms of the transfer function $G(s)$. For this reason, the next lemma is introduced:

Lemma 4: $H(s) \in \{\mathrm{PR}\}$ if and only if $G(s)$ is a phase lead network with maximal phase lead not exceeding 180 deg.

Proof: Recall Eq. (12). Because $\angle H(j\omega) = \angle G(j\omega) - \pi/2$, $H(s) \in \{\mathrm{PR}\}$ if and only if $0 \leq \angle G(j\omega) \leq \pi$. $\square$

In view of the preceding discussion, we may summarize the design guidelines sufficient to avoid output acceleration saturation.

1) Given flight control dynamics $G_1(s)$ and seeker dynamics $G_2(s)$, design a controller $K(s)$ such that $G(s) = K(s)G_1(s)G_2(s)$ is a phase lead network with a maximal phase lead not exceeding 180 deg.

2) Given the missile–target maneuver ratio μ_0, choose N' such that $N'/(N' - 2) \geq \mu_0$, or equivalently $N' \geq 2\mu_0/(\mu_0 - 1)$.

From design guideline 2 it is obvious that the smaller μ_0 is, the larger N' should be chosen.

When following the design guidelines, it is assured that saturation is prevented. Yet, the most obvious question asked is how this design influences the miss distance. It is subsequently shown that L^∞/L^∞ stability is strongly associated with miss distance.

It was proved in previous studies[13,14] that if the guidance system is linear, and in addition

$$H(s) \in \mathbf{Z} \triangleq \{H(s) \mid r[H(s)] = 1\} \tag{48}$$

ZMD will be obtained for any bounded target maneuver. The consequence of Eq. (48) is as follows: If the saturations of the guidance loop remain inactive, then if the degree of the numerator of $G(s)$ equals the degree of the denominator of $G(s)$, ZMD will be obtained for any flight time and any bounded target maneuver. We emphasize that this important theoretical result was rigorously proved in Refs. 13 and 14.

In our case, the nonlinearities embedded in the guidance system are not active, and it is assured that the operating region of the state variables is linear. Hence, we can examine the miss distance utilizing the assumption of linearity, as was done in Refs. 13 and 14. Also, due to Eq. (13), it is clear that

$$\{\mathrm{PR}\} \subseteq \mathbf{Z} \tag{49}$$

that is, the class of transfer functions that guarantees operation in the nonsaturating region is a subset of the class that guarantees ZMD. Thus, if design principles 1 and 2 are followed, not only saturation is prevented, but ZMD shall be rendered. Consequently, the PNG-based systems satisfying design principles 1 and 2 will be called hereafter ZMD–PNG systems. In the sequel, we illustrate the ZMD property by simulation (Sec. VIII.D).

VII. Preventing Saturation of Additional State Variables

The treatment thus far can be repeated in the context of preventing saturation in state variables such as a_C and λ. It is known that for ideal missile dynamics[5]

$$\frac{a_C(t)}{a_T} = \frac{N'}{N'-2}\left[1-\left(1-\frac{t}{t_f}\right)^{N'-2}\right] \tag{50}$$

Consequently, as was the case for a_M, parameter $\mu(\gamma) = N'/(N'-2)$. Thus, if design principles 1 and 2 are followed, commanded acceleration saturation will be avoided as well.

It is also known[5] that for ideal missile dynamics,

$$\frac{\dot\lambda(t)}{a_T} = \frac{1}{V_C(N'-2)}\left[1-\left(1-\frac{t}{t_f}\right)^{N'-2}\right] \tag{51}$$

In this case we have $\mu(\gamma) = 1/V_C(N'-2)$. Without a loss of generality, we can normalize a_T to obtain $\|a_T\|_\infty = 1$. Given the maximal allowed LOS angular rate $\dot\lambda_{\max}$, design guideline 1 remains unchanged. Equivalently to design guideline 2, N' should be chosen as follows:

$$N' \geq 2 + 1/V_C\dot\lambda_{\max} \tag{52}$$

VIII. Illustrative Examples

The design process proposed will be illustrated using a third-order model of $G(s)$. The flight control dynamics are assumed to be a second-order transfer function with damping ζ and natural frequency ω_n, and the seeker LOS measurement dynamics are modeled by a single time lag. As a result, we get

$$G_1(s)G_2(s) = 1\Big/\left[(\tau_1 s+1)\cdot\left(s^2\big/\omega_n^2 + 2\zeta s/\omega_n + 1\right)\right] \tag{53}$$

Let

$$\tau_1 = 0.3\ \text{s}, \qquad \zeta = 0.5, \qquad \omega_n = 10\ \text{rad/s} \tag{54}$$

With missile–target maneuver ratio

$$\mu_0 = 2 \tag{55}$$

According to design principle 1, we should design a controller $K(s)$ such that $G(s) = K(s)G_1(s)G_2(s)$ satisfies $0 \leq \angle G(s) \leq 180$ deg. Consider the following controller:

$$K(s) = \prod_{i=1}^{3}\left(\tau_{Z_i}s+1\right) \tag{56}$$

For simplicity, let $\tau_{Z_i} = \tau_Z$. To minimize noise amplification, the smallest τ_Z should be chosen. A straightforward examination shows that $\tau_Z = 0.23$ satisfies the phase lead requirement. Figure 6 shows the phase plot of $G(s)$ before and after adding the controller. It is seen that the controller shifts the phase plot such that $0 \leq \angle G(s) \leq 58 < 180$ deg. Thus, design principle 1 is satisfied.

Controller (56) shall be called an ideal controller, and the resulting PN-based guidance law will be called ideal ZMD–PNG.

Because $K(s)$ is a PD controller, noise amplification problems might arise. To partially overcome the problem, the following controller is suggested:

$$K(s) = \prod_{i=1}^{3}\frac{\left(\tau_{Z_i}s+1\right)}{\left(\tau_{P_i}s+1\right)} \tag{57}$$

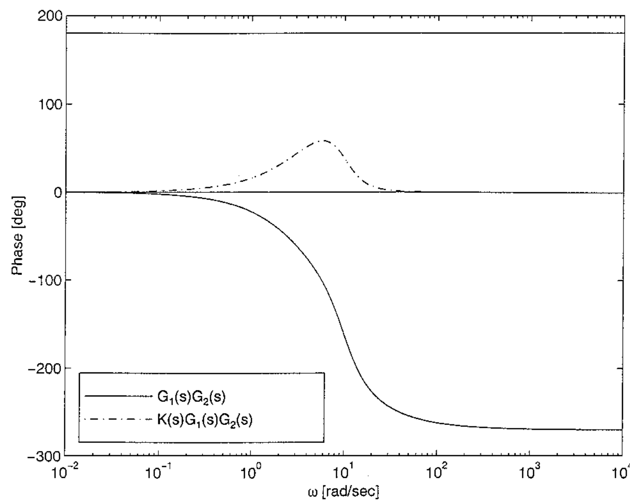

Fig. 6 Phase plot before and after adding a controller.

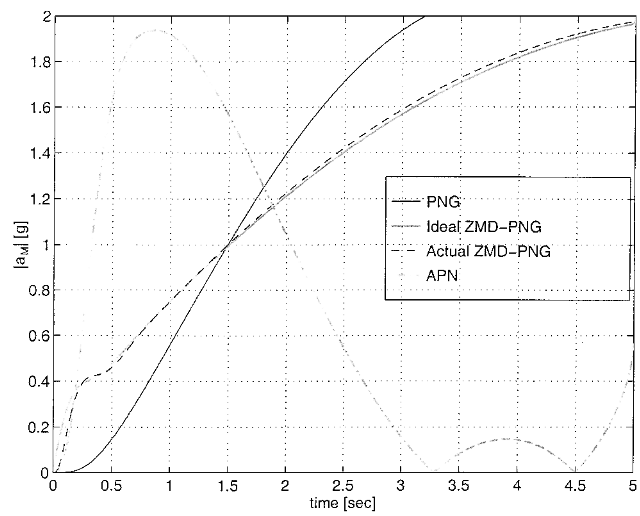

Fig. 7 Maneuver acceleration comparison for a constant target maneuver.

It is apparent that with this type of a controller, design principle 1 cannot be accomplished because Eq. (13) is not satisfied and, hence, $H(s) \notin \{\text{PR}\}$. Nonetheless, if the additional lag is not too large, we can still prevent acceleration saturation. Let $\tau_{P_i} = \tau_P$ and $\tau_{Z_i} = \tau_Z$. If τ_P is small enough, the phase lag will occur at high frequencies, higher than the typical missile operating frequencies. Thus, no substantial degradation of performance is expected although design principle 1 is not fulfilled. We chose the value $\tau_p = 0.05$. Controller (57) shall be called an actual controller, and the resulting PN-based guidance law will be called actual ZMD–PNG.

After designing the appropriate controller, according to design principle 2 it is required that $N' \geq [2.2/(2-1)] = 4$.

The performance of the guidance loop is evaluated in four cases: PNG, ideal ZMD–PNG, actual ZMD–PNG, and augmented PN (APN). Also, we consider three types of target maneuvers: a constant maneuver, a sinusoidal (weave) maneuver, and a random telegraph maneuver.

A. Constant Target Maneuver

Let $a_T = 1\ g$, and $t_f = 5$ s. Figure 7 shows a comparison of the missile maneuver acceleration for the four cases. Notice that when PNG is employed, the acceleration reaches its 2-g limit 2 s before flight end, resulting in a miss of 1 m. However, in the case of ZMD–PNG, no saturation occurs because, $\sup_t |a_M| \leq N'/(N'-2) = 2$. The miss distance is negligible. It is also apparent that the ZMD–PNG performance remains almost unchanged when the ideal case is corrupted by using an additional small lag. The APN presents a fair performance: Although saturation is prevented, the APN requires a larger maneuver effort than the ZMD–PNG.

B. Sinusoidal Target Maneuver

The sinusoidal target maneuver satisfies

$$a_T = a_{T_0} \sin(\omega_T t) \tag{58}$$

Let $a_{T_0} = 1\ g$, $\omega_T = 2.5$ rad/s, and $t_f = 5$ s. Figure 8 shows the absolute value of missile acceleration for the four guidance laws considered. Notice that in the case of PNG, the acceleration saturates, causing a miss distance of 0.5 m. However, ZMD–PNG does not saturate, both in the ideal and actual cases, and the miss distance is negligible. The APN guidance law exhibits a poor performance. It saturates after 2 s and keeps bouncing between the acceleration limits, thus causing a miss distance of 3.1 m. This is because APN is an optimal guidance law for an ideal missile dynamics $[G(s) = 1]$ and a constant target maneuver, which is not satisfied in this example. Hence, APN is not a suitable guidance law for the case discussed.

C. Random Telegraph Maneuver

Recall that a random telegraph maneuver represents a policy, starting at time zero, in which the target executes either a maximum positive or negative acceleration $\pm a_T$ such that the number of sign changes per second follows a Poisson distribution and the average number of sign changes is ν per second. Let $a_T = 1\ g$, $\nu = 1$, and $t_f = 5$ s. Figure 9 shows the absolute value of missile acceleration for the four guidance laws considered. Some interesting observations can be drawn from Fig. 9. PNG saturates 0.5 s before flight termination. The ideal ZMD–PNG does not saturate. Consequently, although deterministic target maneuvers were considered in the analysis, it is evident that, even in case of a random target maneuver, such as random telegraph, the new guidance law prevents missile acceleration saturation. When a small lag is used, that is, actual ZMD–PNG, the acceleration saturates very close to flight termination, thus causing a negligible miss distance. APN does not exhibit a feasible performance; as was mentioned in Sec. VIII.B, this guidance law cannot deal adequately with nonconstant maneuvers when the missile dynamics is nonideal.

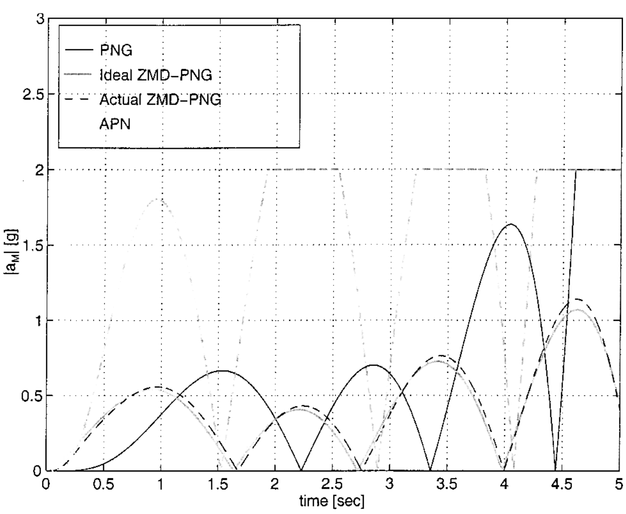

Fig. 8 Maneuver acceleration comparison for a sinusoidal target maneuver.

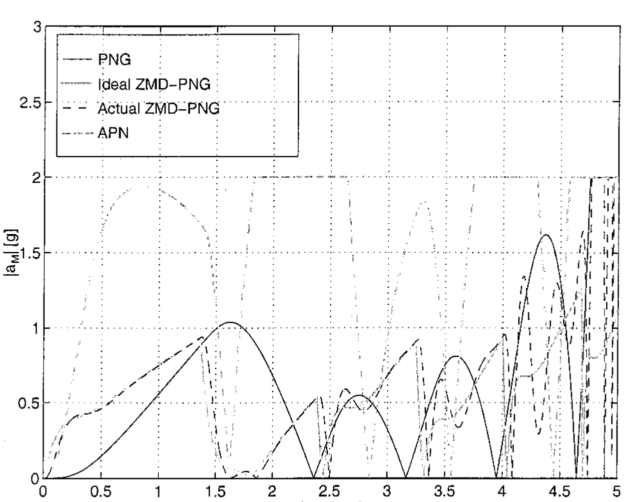

Fig. 9 Maneuver acceleration comparison for a random telegraph target maneuver.

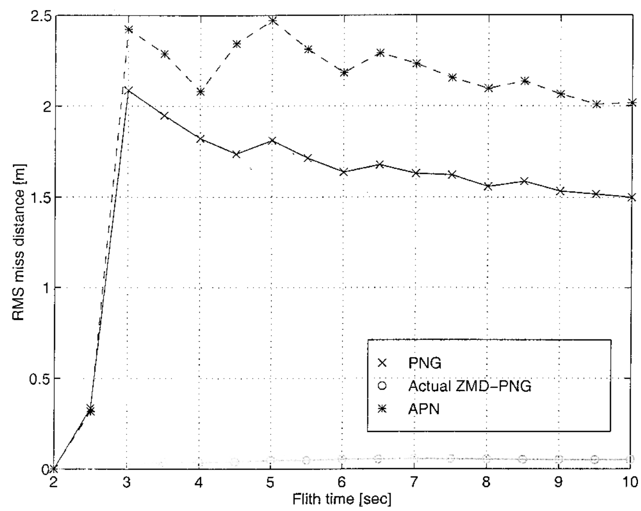

Fig. 10 Comparison of rms miss distance shows that actual ZMD–PNG gives negligible miss distance against a target performing a random-telegraph maneuver.

D. Miss Distance Analysis

It was mentioned earlier that ZMD–PNG in its ideal form induces ZMD. This shall be illustrated using a Monte Carlo simulation designed to examine miss distance statistically as a function of flight time. In the Monte Carlo simulation we assumed a random-telegraph target maneuver with the parameter values assumed in Sec. VIII.C and the missile model given in Eqs. (53–56). To evaluate the ZMD–PNG performance in a stochastic environment, a zero-mean Gaussian white noise with a standard deviation of 0.05 deg/s was added to the LOS measurement. The guidance laws considered were PNG; actual ZMD–PNG, that is, ZMD–PNG with a small lag to account for noise [see Eq. (57)]; and APN. Figure 10 shows rms values of miss distance as a function of flight time. It is seen that PNG yields miss distances that range from 1.5 to 2 m. APN exhibits a worse performance, with a miss ranging from 2 to 2.5 m. However, actual ZMD–PNG yields a small miss, of about 0.05 m. The miss distance with actual ZMD–PNG is not identically zero because of the small lag incorporated to deal with noise filtering. Thus, we conclude that the ZMD–PNG considerably improves miss distance, even when the target maneuver is of random type and the LOS measurement is corrupted by noise.

IX. Conclusions

This paper presented a simple improvement to the well-known PNG law that assured that saturation of maneuver acceleration or other limited state variables was prevented. Based on previous studies and an illustrative example, it was shown that preventing saturation yields ZMD. The improved guidance, called ZMD–PNG, was based on the assumption that the target maneuver was bounded. ZMD–PNG offered two design guidelines to follow: First, the total dynamics of the guidance system should be designed PR. Second, the effective PN constant should be chosen according to a simple function of the given missile–target maneuver ratio. The new guidance law exhibited a significant improvement compared to PNG. The main disadvantage of the proposed law is that it might increase noise sensitivity. However, this obstacle could be overcome by introducing some lag into the system. Some examples illustrated that the new guidance law is robust to small deviations from the design guidelines. Illustrative examples have validated the analysis, showing that a considerable improvement in miss distance could be obtained. This is true both for deterministic and random target maneuvers.

References

[1]Rusnak, I., and Meir., L., "Optimal Guidance for High Order and Acceleration Constrained Missile," *Journal of Guidance, Control, and Dynamics*, Vol. 14, No. 3, 1991, pp. 589–596.

[2]Rusnak, I., "Advanced Guidance Laws for Acceleration Constrained Missile, Randomly Maneuvering Target and Noisy Measurement," *Transactions of the IEEE Regional Conference on Aerospace Control Systems*, Inst. of Electrical and Electronics Engineers, New York, 1993, pp. 453–462.

[3]Gutman, S., "On Optimal Guidance for Homing Missiles," *Journal of Guidance and Control*, Vol. 2, No. 4, 1979, pp. 296–300.

[4]Shneydor, N., *Missile Guidance and Pursuit*, Horwood, West Sussex, England, UK, 1998, Chap. 5, pp. 101–124.

[5]Zarchan, P., *Tactical and Strategic Missile Guidance*, Vol. 124, Progress in Astronautics and Aeronautics, AIAA, Washington, DC, 1990, Chap. 2, pp. 17–35.

[6]Shinar, J., "Divergence Range of Homing Missiles," *Israel Journal of Technology*, Vol. 14, July 1976, pp. 47–55.

[7]Gurfil, P., Jodorkovsky, M., and Guelman, M., "Finite Time Stability Approach to Proportional Navigation Systems Analysis," *Journal of Guidance, Control, and Dynamics*, Vol. 21, No. 6, 1998, pp. 853–861.

[8]Shinar, J., and Steinberg, D., "Analysis of Optimal Evasive Maneuvers Based on a Linearized Two-Dimensional Kinematic Model," *Journal of Aircraft*, Vol. 14, No. 8, 1977, pp. 795–802.

[9]Zarchan, P., "Complete Statistical Analysis of Nonlinear Missile Guidance Systems-SLAM," *Journal of Guidance and Control*, Vol. 2, No. 1, 1979, pp. 71–78.

[10]Sandberg, I. W., "Some Results on the Theory of Physical Systems Governed by Nonlinear Functional Equations," *Bell Systems Technology Journal*, Vol. 44, No. 5, 1965, pp. 871–898.

[11]Zames, G., "On Input–Output Stability of Time-Varying Nonlinear Feedback Systems—Part II: Conditions Involving Circles in the Frequency Plane and Sector Nonlinearities," *IEEE Transactions on Automatic Control*, Vol. AC-11, 1966, pp. 465–476.

[12]Mossaheb, S., "The Circle Criterion and the L^P Stability of Feedback Systems," *SIAM Journal on Control and Optimization*, Vol. 20, No. 1, 1982, pp. 144–151

[13]Gurfil, P., Jodorkovsky, M., and Guelman, M., "Simple Guidance Law Against Highly Maneuvering Targets," *Proceedings of the 38th AIAA Guidance, Navigation, and Control Conference*, AIAA, Reston, VA, 1998, pp. 570–580.

[14]Gurfil, P., Jodorkovsky, M., and Guelman, M., "Design of Zero Miss Distance Proportional Navigation Guidance Systems" (submitted for publication).

[15]Desoer, C. A., and Vidyasagar, M., *Feedback Systems: Input–Output Properties*, Academic, New York, 1975, Chap. 2, pp. 42–55.

[16]Doyle, J. C., Francis, B. A., and Tannenbaum, A. R., *Feedback Control Theory*, Macmillan, New York, 1992, Chap. 2, pp. 13–31.

[17]Slotine, J. J. E., and Li, W., *Applied Nonlinear Control*, Prentice–Hall, Upper Saddle River, NJ, 1991, Chap. 4, pp. 128–143.

[18]Sandberg, I. W., and Johnson, K. K., "Steady State Errors and the Circle Criterion," *IEEE Transactions on Automatic Control*, Vol. 35, No. 1, 1990, pp. 530–534.

[19]Sandberg, I. W., "A Frequency Domain Condition for the Stability of Feedback Systems Containing a Single Time-Varying Nonlinear Element," *Bell Systems Technical Journal*, Vol. 43, 1964, pp. 1601–1608.